

# Magnetic Excitations of Coupled Spin Ladders: a Quantum Monte Carlo Study

Brian M. Andersen<sup>1</sup> and Olav F. Syljuåsen<sup>2</sup>

<sup>1</sup>*Department of Physics, University of Florida, Gainesville, Florida 32611-8440, USA*

<sup>2</sup>*NORDITA, Blegdamsvej 17, DK-2100 Copenhagen Ø, Denmark*

(Dated: January 7, 2019)

We calculate the magnetic excitation spectrum in the stripe phase of high- $T_c$  materials. The stripes are modeled as coupled spin-1/2 ladders and the spin dynamics is extracted using Quantum Monte Carlo (QMC) simulations, which can capture the strong quantum fluctuations near quantum critical points of coupled spin ladders. We find a characteristic hourglass magnetic excitation spectrum with high-energy peaks rotated by 45 degrees compared to the incommensurate low-energy peaks in good agreement with the experimental data. The excitations are investigated quantitatively as a function of interladder coupling, ladder width, and domain formation with stripe disorder.

PACS numbers: 74.25.Ha, 75.40.Gb, 75.10.Jm, 75.40.Mg

Neutron scattering experiments are powerful probes of the bulk spin excitations of magnetic materials, and has been applied extensively to the cuprates since their discovery[1]. However, only recently have observations of universal fluctuations been reported[2, 3], providing a crucial new piece of information for the general understanding of how these materials evolve from an antiferromagnetic (AF) Mott insulator to a  $d$ -wave superconductor as electrons are extracted from the  $\text{CuO}_2$  planes.

There is increasing evidence that competing interactions in the cuprate materials result in spatially inhomogeneous electronic spin and charge ground states in a significant region of the phase diagram, and it is important to determine whether experimental bulk probes are in agreement with such inhomogeneous solutions in general, and one-dimensional stripe configurations in particular[4]. While it might be tempting to model the magnetic response by checkerboard order[5], it is well-known that such textures cannot reproduce the data[6]. A recent neutron study of  $\text{La}_{1.48}\text{Nd}_{0.4}\text{Sr}_{0.12}\text{CuO}_4$  has confirmed that indeed the magnetic order is collinear and modulated one-dimensionally consistent with stripes[7].

Recent extensive neutron scattering experiments on several cuprate materials have been performed to map out the details of the magnetic fluctuations over a large energy range[2, 3, 8, 9, 10]. The compound  $\text{La}_{1.875}\text{Ba}_{0.125}\text{CuO}_4$  (LBCO) is known to support static stripe spin and charge order below  $T = 50\text{K}$  as indicated by superlattice Bragg peaks in both sectors[11]. The low-energy magnetic excitation spectrum of this material[2] (at  $T > T_c$ ) consists of inwardly dispersing incommensurate spin branches. In  $\text{La}_{2-x}\text{Sr}_x\text{CuO}_4$  (LSCO) the momentum position of similar incommensurate modes are known to scale linearly with the doping up to  $\sim \frac{1}{8}$ , a property that is naturally explained within the stripe scenario[12, 13]. For LBCO the low-energy branches merge into the "resonance point" at  $(\pi, \pi)$  at an energy close to 50 meV. At even higher energies, constant energy cuts reveal that the excitations disperse outward and form a square or ring feature with four prominent peaks

rotated by 45 degrees compared to the low-energy incommensurate modes. The resulting spin response exhibits a characteristic hourglass shape, and is remarkably similar to the data obtained in LSCO[14] and  $\text{YBa}_2\text{Cu}_3\text{O}_{6+x}$  (YBCO) [3, 8, 10, 15, 16, 17, 18]. This supports the notion of a universal spin spectrum[19] modulo various quantitative differences, particularly at low energies resulting from e.g. material dependent exchange couplings, quasiparticle damping effects, and possible existence of a doping and temperature dependent spin gap.

Theoretically, several groups have used various spin-only models to compute semiclassically the magnetic excitations in stripe states with magnetic long-range order (LRO)[19, 20, 21]. It has, however, been pointed out that strong quantum fluctuations are important for obtaining the correct high-energy response originating from the quasi-one-dimensional spin excitations of the ladder[2, 22, 23, 24], even though, in certain limits, the magnetic fluctuations can closely resemble the semiclassical results[25]. The importance of the charges in describing the spin response remains controversial, but is expected to affect the details at low energy as mentioned above. The charge degrees of freedom have been included within phenomenological models[26], and within time-dependent Gutzwiller approximation of the Hubbard model[24]. The coexistence phase of static stripes and  $d$ -wave superconductivity was studied in Ref. 27 using a mean-field+RPA approximation.

In this paper, motivated by the discovery of universal spin fluctuations, we calculate the dynamical structure factor  $S(\mathbf{q}, \omega)$  with a powerful QMC method able to treat both the ordered and quantum disordered regimes. We discuss effects of interladder coupling, ladder width, and disorder. As opposed to previous microscopic spin-only models, we do not rely on semiclassical linearized spin-wave[19, 20, 21, 25], or one-tripion[23] approximations.

The spin dynamics is qualitatively different in isolated even and odd leg spin-1/2 ladders[28]; whereas even leg ladders display a spin gap and short-range spin-spin correlations, the odd leg ladders are qualitatively similar to

the spin-1/2 chain with gapless quasi-long-range correlations. For coupled ladders, the odd leg ladders support an ordered state for any interladder exchange coupling  $J_b$ , whereas coupled even leg ladders exhibit a quantum critical point (QCP) at some finite value of  $J_b$ [29]. For the cuprates, at a doping near  $x = \frac{1}{8}$  the charge is modulated with a period close to four lattice constants, half the period of the associated spin modulations. Hence, the associated stripe phase may consist of coupled 2-, 3-, or 4-leg spin ladders containing 2, 1, and 0 spin-empty sites, respectively. In the following, the spins on the Cu atoms in the  $\text{CuO}_2$  planes are modeled by the Heisenberg Hamiltonian defined on a square lattice

$$\mathcal{H} = \sum_{\langle ij \rangle} J_{ij} \mathbf{S}_i \cdot \mathbf{S}_j, \quad (1)$$

where  $\mathbf{S}_i$  is the spin-1/2 operator at site  $i$ , and  $J_{ij}$  denotes the exchange coupling between sites  $i$  and  $j$ . Unidirectional stripes parallel to the  $y$ -axis are modeled by couplings  $J_b$  across the hole-rich quasi-one-dimensional regions and  $J_a$  elsewhere[30]. The Hamiltonian (1) and the assumed stripy configurations of exchange couplings is the resulting effective spin-only model after integrating out the charge carriers. Whereas  $J_a > 0$ , the sign of  $J_b$  depends on the period of the stripes:  $J_b > 0$  for site-centered stripes and  $J_b < 0$  for bond-centered stripes[25]. The choices accommodate the anti-phase property of the stripes believed to originate from a lowering of the kinetic energy of the carriers. Below, we study  $L \times L$  lattices with periodic boundary conditions, and use tetragonal units with wave vectors  $q_x, q_y$  parallel to the Cu-O bonds, and energies are given in units of  $J_a$ . We typically set  $L = 64$  allowing us to study momentum resolved correlations functions within QMC.

The QMC simulations were performed using the Stochastic Series Expansion (SSE) method[31] with directed-loop updates[32]. In order to extract imaginary-time correlation functions the individual vertices in an SSE configuration were each assigned a random imaginary-time location in such a way that the assignment did not alter the imaginary-time ordering sequence of vertices[33]. The  $\langle S_i^z(\tau) S_j^z(0) \rangle$  correlation function was read out using a mesh with 200 grid points along the imaginary-time axis and Fast Fourier transforms were used to obtain the momentum space points. The imaginary-time data was finally continued to real-frequency using the MaxEnt method[34] with a flat prior.

Fig. 1 shows superimposed results for  $S(\mathbf{q}, \omega)$  as a function of energy  $\omega$  and momenta along cuts  $(q_x, \pi)$  and  $(\pi, q_y)$  for coupled 2- (a), 3- (b) and 4-leg ladders (c), all with  $|J_b| = 0.1$  for easy comparison. For this value of  $J_b$  the coupled 2-leg ladders are in the quantum disordered regime and displays a gap as seen in 1(a), whereas magnetic LRO and Goldstone modes exist for the coupled 3- and 4-leg ladders. Fig. 1(a-c) clearly show an hourglass spin spectrum consisting of anisotropic low-energy

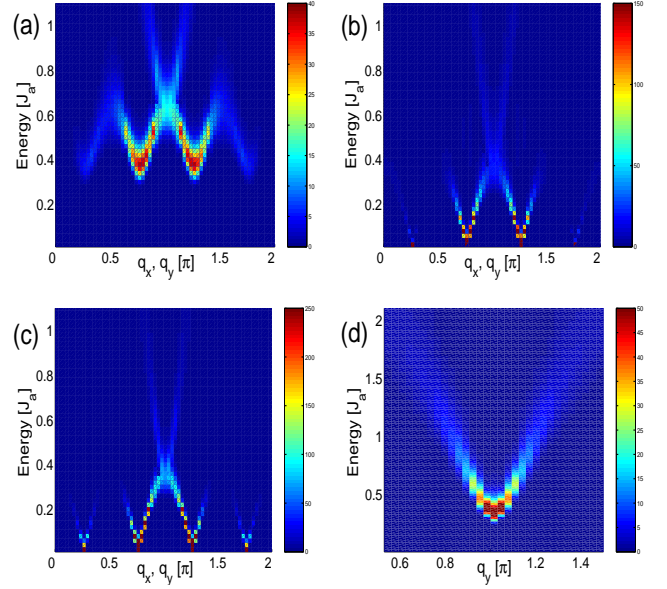


FIG. 1: (Color online) (a-c)  $S(q_x, \pi, \omega)$  vs  $q_x$  superimposed with  $S(\pi, q_y, \omega)$  vs  $q_y$  showing the characteristic X-shaped hourglass spin excitation spectrum for coupled 2- (a), 3- (b), and 4-leg ladders (c) with  $|J_b| = 0.1$  and  $J_a \beta = 80$ . (d)  $S(\pi, q_y, \omega)$  vs  $q_y$  from (c) showing the high-energy quasi 1D dispersion along the 4-leg spin ladder (note different scale). In (b,c) the amplitude of peaks at  $(1 \pm \frac{3}{4})\pi$  are reduced by an order of magnitude compared to the main peaks at  $(1 \pm \frac{1}{4})\pi$ .

spin modes and a dispersive high-energy branch characteristic of quasi-one-dimensional quantum paramagnets, as shown separately in Fig. 1(d). Important features in Fig. 1 are the energy  $\omega_\pi$  of the saddle point in the dispersion at  $(\pi, \pi)$  (resonance point), and the minimum gap  $\Delta$  at  $(1 \pm \frac{1}{4})\pi$ . Fig. 2(a) shows the resonance energy  $\omega_\pi$  for the 2-, 3-, and 4-leg ladders as a function of the interladder coupling  $|J_b|$ . As seen,  $\omega_\pi$  increases with  $|J_b|$ , and the even leg ladders display a gap at  $J_b = 0$  as expected. Note that for the 3-leg ladder  $\omega_\pi$  does not vanish identically at  $J_b = 0$  due to the finite temperature. This agrees with  $\sigma$ -model calculations which give  $\omega_\pi = \pi T + \dots$ , where ellipses denote higher order logarithmic corrections[35].

The intensity anisotropy ratio  $R_I$  between the inner (toward  $(\pi, \pi)$ ) and outer (away from  $(\pi, \pi)$ ) branches of the low-energy modes is another important quantity since the outer branches are not yet observable in experiments. We define an anisotropy ratio by  $R_I = [S(q_B + q_I, \pi) - S(q_B - q_I, \pi)] / S(q_B + q_I, \pi)$  where  $S(\mathbf{q})$  is the energy integrated structure factor, and  $q_I = |q_B - q_x|$  with  $q_B = 3\pi/4$  one of the Bragg points. Fig. 2(b-d) show  $R_I$  vs  $q_I$  for the coupled 2-, 3-, and 4-leg ladders for various values of  $J_b$ . Clearly  $R_I$  decreases with increasing interladder coupling[25], and for the 2-leg ladders  $R_I$  remains small ( $\lesssim 15\%$ ) in the vicinity of the Bragg point for all  $J_b$ . In fact, based only on  $R_I$  one would expect the 4-leg ladders to best model

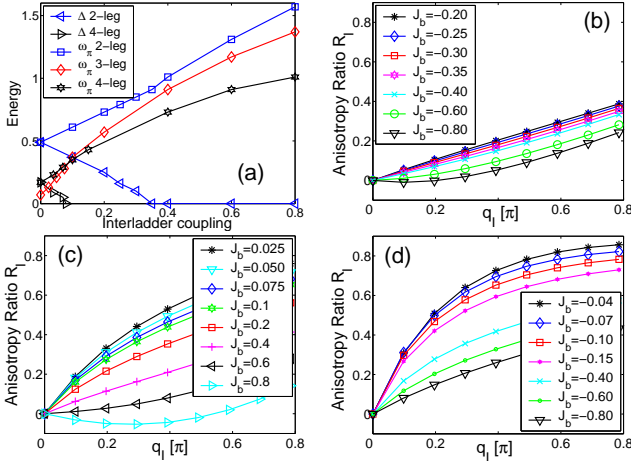


FIG. 2: (Color online) (a) Resonance  $\omega_\pi$  and mode gap  $\Delta$  at  $3\pi/4$  vs interladder coupling  $J_b$ . (b-d) The anisotropy ratio  $R_I$  vs  $q_l = |q_B - q_x|$  for coupled 2- (b), 3- (c), and 4-leg ladders (d). All results are obtained with  $J_a\beta = 40$  and  $L = 64$ .

the experiments[8, 9, 10, 11, 14, 15, 16, 17, 18]. For large enough  $J_b$ ,  $R_I$  eventually becomes negative and the outer branches dominate the intensity. We have also studied coupled 6- and 8-leg ladders, and found excitations qualitatively similar to Fig. 1(b-c) but with even larger anisotropy ratios between the inner and outer low-energy spin branches.

Fig. 3 shows constant energy cuts of  $S(\mathbf{q}, \omega)$  for the coupled 4-leg ladders with the same parameters as in Fig. 1(c-d). Similar to experiments, with increasing energy the incommensurate low-energy peaks merge at the resonance point around  $\sim 0.3$  and the high-energy response consists of a diamond structure dominated by four peaks rotated 45 degrees compared to the ones at low energy. In Fig. 4 we show the momentum integrated structure factor  $S(\omega)$  for the same parameters used in Fig. 1. Besides the  $\omega = 0$  Bragg peak (for the ordered cases),  $S(\omega)$  is dominated by two characteristic peaks corresponding to the saddle point in the dispersion at the resonance point, and a peak at the upper band edge of the dispersive branch along the ladders ( $\omega \sim 2J_a$ ).

Important open questions relates to the effects of disorder and stripe domain formation on the magnetic excitations, and the origin of the spin gap. In LSCO magnetic LRO is observed at low doping  $x \lesssim 0.14$ [12, 36], whereas at higher doping a spin gap phase, which may be related to superconductivity, opens up. YBCO and BSCCO exhibit a large spin gap, i.e. the stripes remain fluctuating at all doping levels possibly related to a smaller interladder coupling  $J_b$  leaving these materials in the quantum disordered regime. Within a phenomenological approach Vojta *et al.*[37] recently studied the spin susceptibility in the presence of slow dynamically fluctuating charge stripes. As a further complexity there is also evidence from muon spin relaxation experiments that LSCO and

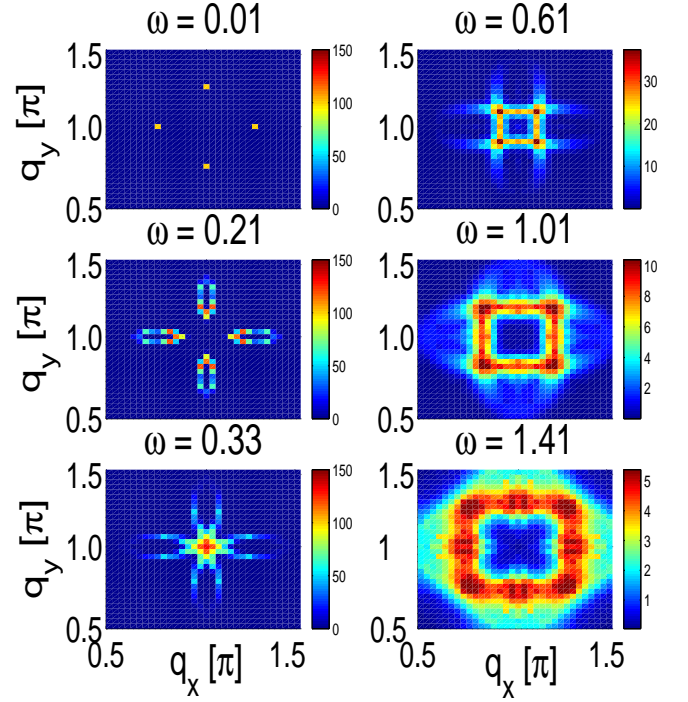


FIG. 3: (Color online) Constant energy cuts of  $S(\mathbf{q}, \omega)$  for coupled 4-leg ladders;  $J_b = -0.1$ ,  $L = 64$ , and  $J_a\beta = 80$ . Similar results can be generated for coupled 2- and 3-leg ladders but with reduced anisotropy ratios  $R_I$  (Fig. 2).

YBCO exhibit a spin-glass phase with local 'static' short-range order.

In the rest of this paper, we wish to study a simple disorder scenario which simulates both random stripe positions and finite sized stripe domains. Domain formation was an assumption when symmetrizing the plots in Figs. 1 and 3, and should be a natural consequence of

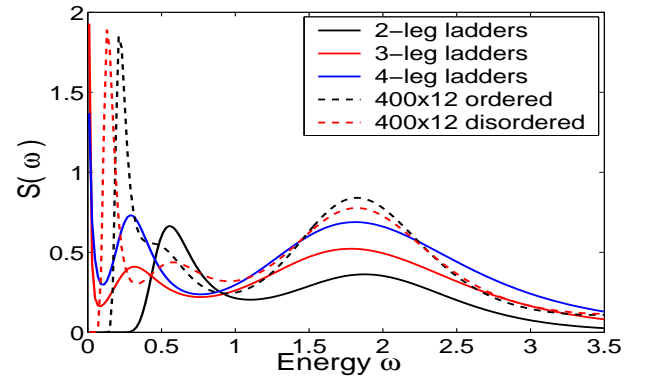


FIG. 4: (Color online)  $S(\omega)$  for coupled 2- (black) 3- (red) and 4-leg (blue) ladders with parameters similar to Fig. 1. Dashed lines show the results for  $400 \times 12$  sites with ordered (black) and disordered (red) 4-leg ladders ( $J_b = -0.1$ ).

random quenched disorder[38]. In the following we simulate this kind of disorder by studying systems of size  $400 \times L$  where  $L$  is an assumed average domain size, and the stripe positions are disordered with a flat distribution in the interval [1,7] (mean 4). Clearly this approach is crude, but has been successfully applied to explain the quasiparticle spectral weight as detected by photoemission spectroscopy[39]. In general, we find that this kind of disorder is very detrimental to the hour-glass excitations *unless*  $L$  is small enough to induce a spin gap. For example, for  $400 \times 12$  systems with parameters similar to Fig. 3, we show in Fig. 5 the result for ordered (a) and disordered (b) stripes. The disordered case is averaged over 4 different configurations which is enough for these large systems. The corresponding  $S(\omega)$  are shown in Fig. 4. Fig. 5 demonstrates a case of domain-induced spin gap which is a property of the individual  $4 \times 12$  clusters that (when coupled) constitute the system (a gap is negligible in the  $64 \times 64$  system (Fig. 3), and in  $400 \times 12$  systems with  $J_b \sim J_a$  (not shown)). Interestingly, as seen from Fig. 5(b), the stripe disordering not only smears the excitation spectrum resulting in diffuse 'legs of scattering', but also strongly reduces the spin gap. In this case the resulting pile-up of weight right above the spin gap is clearly unrelated to (but may be enhanced by[27]) superconductivity. We expect this scenario to be most relevant for LSCO[14], whereas in YBCO, where the intensity is peaked near  $(\pi, \pi)$ , fluctuating charge stripes[37] or superconductivity[27] may be important. For this material, however, it remains controversial whether homogeneous models are better starting points, at least for the optimally-to overdoped regime[40, 41].

In summary, we have calculated the spin excitations in the stripe phase within a Heisenberg model of coupled spin ladders using QMC, and investigated the effects of interladder coupling, ladder width and simple types of disorder. In agreement with experiments, we find low-energy spin-wave like excitations with intensity strongly dominated by the inner branches for low interladder coupling. These merge at the  $(\pi, \pi)$  point and rotate into the quantum excitations characteristic of the quasi-one-

dimensional spin ladders at higher energies.

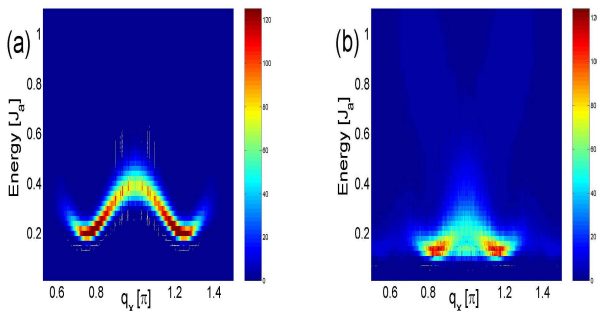


FIG. 5: (Color online) "Boomerang" excitation spectrum for a  $400 \times 12$  system of ordered (a) and disordered (b) stripes.

- [1] For a review see, J. M. Tranquada, cond-mat/0512115.
- [2] J. Tranquada *et al.*, Nature (London) **429**, 534 (2004).
- [3] S. M. Hayden *et al.*, Nature (London) **429**, 531 (2004).
- [4] S. A. Kivelson *et al.*, Rev. Mod. Phys. **75**, 1201 (2003).
- [5] T. Hanaguri *et al.*, Nature **430**, 1001 (2004).
- [6] B. M. Andersen, P. Hedegård, and H. Bruus, Phys. Rev. B **67**, 134528 (2003).
- [7] N. B. Christensen *et al.*, cond-mat/0608204.
- [8] C. Stock *et al.*, Phys. Rev. B **69**, 014502 (2004).
- [9] V. Hinkov *et al.*, Nature **430**, 650 (2004).
- [10] S. Pailhès *et al.*, Phys. Rev. Lett. **93**, 167001 (2004).
- [11] M. Fujita *et al.*, Phys. Rev. B **70**, 104517 (2004).
- [12] K. Yamada *et al.*, Phys. Rev. B **57**, 6165 (1998).
- [13] J. Lorenzana and G. Seibold, cond-mat/0606411.
- [14] N. B. Christensen *et al.*, Phys. Rev. Lett. **93**, 147002 (2004).
- [15] M. Arai *et al.*, Phys. Rev. Lett. **83**, 608 (1999).
- [16] P. Bourges *et al.*, Science **288**, 1234 (2000).
- [17] H. Mook, P. C. Dai, and F. Dogan, Phys. Rev. Lett. **88**, 097004 (2002).
- [18] D. Reznik *et al.*, Phys. Rev. Lett. **93**, 207003 (2004).
- [19] C. D. Batista, G. Ortiz, and A. V. Balatsky, Phys. Rev. B **64**, 172508 (2001).
- [20] F. Krüger and S. Scheidl, Phys. Rev. B **67**, 134512 (2003).
- [21] E. W. Carlson, D. X. Yao, and D. K. Campbell, Phys. Rev. B **70**, 064505 (2004).
- [22] M. Vojta and T. Ulbricht, Phys. Rev. Lett. **93**, 127002 (2004).
- [23] G. S. Uhrig, K. P. Schmidt, and M. Grüninger, Phys. Rev. Lett. **93**, 267003 (2004).
- [24] G. Seibold and J. Lorenzana, Phys. Rev. Lett. **94**, 107006 (2005).
- [25] D. X. Yao, E. W. Carlson, and D. K. Campbell, Phys. Rev. Lett. **97**, 017003 (2006).
- [26] M. Vojta and S. Sachdev, J. Phys. Chem. Solids, **67**, 11 (2006).
- [27] B. M. Andersen and P. Hedegård, Phys. Rev. Lett. **95**, 037002 (2005).
- [28] E. Dagotto and M. Rice, Science **271**, 618 (1996).
- [29] Y. J. Kim *et al.*, Phys. Rev. B **60**, 3294 (1999).
- [30] S. Dalosto and J. Riera, Phys. Rev. B **62**, 928 (2000).
- [31] A. W. Sandvik and J. Kurkijärvi, Phys. Rev. B **43**, 5950 (1991).
- [32] O. F. Syljuåsen and A. W. Sandvik, Phys. Rev. E **66**, 046701 (2002).
- [33] A. W. Sandvik, R. R. P. Singh, and D. K. Campbell, Phys. Rev. B **56**, 14510 (1997).
- [34] R. N. Silver, D. S. Sivia, and J. E. Gubernatis, Phys. Rev. B **41**, 2380 (1990); W. von der Linden, Appl. Phys. A **60**, 155 (1995).
- [35] O. F. Syljuåsen, Int. J. Mod. Phys. B **14**, 457 (2000).
- [36] J. Tranquada *et al.*, Nature (London) **375**, 561 (1995).
- [37] M. Vojta, T. Vojta, and R. K. Kaul, cond-mat/0510448.
- [38] J. A. Robinson *et al.*, cond-mat/0602675; A. Del Maestro, B. Rosenow, and S. Sachdev, cond-mat/0603029.
- [39] M. Granath *et al.*, Phys. Rev. B **65**, 184501 (2002).
- [40] D. Manske *et al.*, Phys. Rev. B **63**, 054517 (2001).

- [41] I. Eremin *et al.*, Phys. Rev. Lett. **94**, 147001 (2005).